applied sciences

MDPI

Article

Influence of Seismic Loads Considering Soil Properties and Wave Passage Effect on the Seismic Response of a Multi-Span PSC Girder Bridge

Gun Park [1], Yeong-Mo Yeon [2,*], Ki-Nam Hong [2] and Sugyu Lee [3]

[1] Earthquake Hazards Reduction Center, National Disaster Management Research Institute, 406-33, Jongga-ro, Jung-gu, Ulsan 44538, Korea; parkgun1@korea.kr
[2] Department of Civil Engineering, Chungbuk National University, 1 Chungdae-ro, Seowon-gu, Cheongju 28644, Korea; hong@chungbuk.ac.kr
[3] Land and Housing Institute, 99, Expo-ro 539, Yuseong-gu, Daejeon 34047, Korea; glee@lh.or.kr
* Correspondence: yym235@chungbuk.ac.kr

Abstract: This paper investigates the analytical results of the seismic response of multi-span prestressed concrete (PSC) I-girder bridges under seismic loads. To perform numerical analyses, a three-span PSC I-girder bridge with a width of 12 m, a total length of 100 m, and a maximum span length of 40 m was modeled, and a virtual location was selected to consider the soil properties of the area where the bridge was constructed. The seismic load acting on the PSC I-girder bridge was applied in consideration of the soil properties around the pier and the wave passage effect of the bedrock in the artificial seismic load generated, according to the U.S. Nuclear Regulatory Commission (NRC) standard. The analysis results confirmed that the seismic load, with consideration of the soil properties and wave passage effect, generated the maximum response acceleration and bending moment at the deck of the bridge—152% and 232% greater than without considering them, respectively. Therefore, in order to ensure the earthquake resistance of the bridge, the soil properties of the area where the bridge will be built and the wave passage effect of the bedrock must be considered.

Keywords: wave passage effect; PSC girder bridge; seismic analysis

Citation: Park, G.; Yeon, Y.-M.; Hong, K.-N.; Lee, S. Influence of Seismic Loads Considering Soil Properties and Wave Passage Effect on the Seismic Response of a Multi-Span PSC Girder Bridge. *Appl. Sci.* **2022**, *12*, 1415. https://doi.org/10.3390/app12031415

Academic Editor: Roberto Nascimbene

Received: 3 January 2022
Accepted: 26 January 2022
Published: 28 January 2022

1. Introduction

The Circum-Pacific belt, also known as the Ring of Fire, has recently been active, so earthquakes of varying intensity are frequently occurring in various regions around the world. Earthquakes such as the 2001 Indian Gujarat earthquake, the 2005 Pakistan earthquake, the 2008 Sichuan earthquake, and the 2011 East Japan earthquake have caused 200,000 casualties and caused enormous loss of life and property [1–3]. In addition, the increased frequency of strong earthquakes raises questions about whether existing infrastructure is sufficiently safe from strong earthquakes.

Infrastructure such as bridges, dams, and nuclear power plants requires a lot of time and money to plan, design, and construct. In addition, such infrastructure plays an important role in a nation's economy, including transportation of goods, electricity production, and preparedness for droughts and floods. If such infrastructure is damaged by earthquakes, it can have a huge impact on the national economy, beyond the structures simply not functioning properly. Therefore, ensuring the earthquake resistance of such infrastructure should be considered extremely important.

The seismic capacity of infrastructure should be evaluated comprehensively, considering not only their strength and deformability, but also the soil–structure interaction (SSI), which is the mutual interaction between soil (ground) and a structure built on it [4]. This is because seismic waves generated from bedrock increase in peak acceleration and change in natural frequency depending on the properties of the soil. The earthquake that occurred in Mexico City in 1985 is a representative example [5]. Therefore, recent studies related to the seismic response of structures are necessarily conducted in consideration of the soil's essential properties [6–12].

The seismic wave travels through the bedrock with a time difference due to the shear wave velocity of the bedrock, which causes a difference in the characteristics of the seismic load that accelerates the ground on which the foundation of the structure is placed. In particular, the wave passage effect cannot be ignored when the bedrock is extremely deep or is not sufficiently hard [13–17]. Therefore, the wave passage effect of earthquakes is an important consideration in the seismic design of a variety of long infrastructure such as bridges, pipelines, and tunnels [18].

The purpose of this study was to investigate the seismic response of a bridge with multiple supports under seismic loads, considering both the soil properties of the area where the bridge was constructed and the wave passage effect. To this end, the seismic load acting on the bedrock was prepared to meet the design criterion presented in the standard of the U.S. NRC. In order to reflect the soil properties of the area where the piers are installed in the initial seismic load generated in this way, a ground response analysis was performed using DEEPSOIL—a site response analysis program. Furthermore, the wave passage effect was reflected by considering the shear wave velocity of the bedrock for each support. Prior studies on the seismic response of bridges during earthquakes have been conducted by applying each parameter individually [19–23], but studies that consider both the amplification and the wave passage effect of seismic waves due to the soil characteristics are insufficient. Therefore, in this study, the seismic response of the bridge during earthquakes was investigated by considering both soil properties in the area where the bridge is located and the wave passage effect of the seismic wave at each support. Figure 1 shows an overall flowchart of the analysis performed in this study.

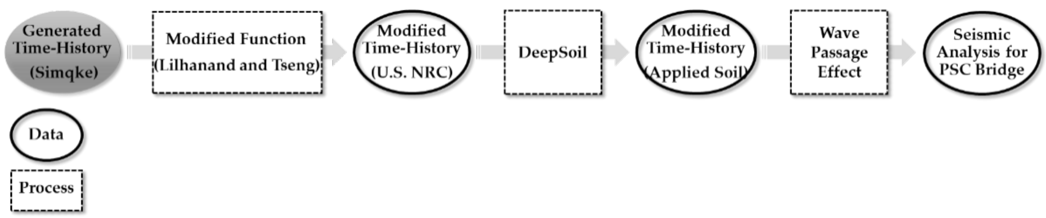

Figure 1. Overview of the seismic analysis for a PSC girder bridge.

2. Background

A pre-stressed concrete (PSC) girder bridge is a type of bridge in which a slab is placed on an I-shaped pre-stressed concrete girder; most of them are applied to spans of 20 to 40 m, and they are the most widely used because their construction cost is lower than that of girder bridges made of steel. In particular, PSC I-girders are mainly used to construct highway bridges or bridges that pass over streams, where the length between piers does not exceed 40 m and there is no restriction on the space under the bridge. In this study, a virtual PSC girder bridge and the area where it would be constructed were set up; a general PSC I-girder bridge is shown in Figure 2.

When evaluating the dynamic response of a bridge during an earthquake, the most important factor to be considered is the seismic load acting on the bridge. Prior studies were conducted experimentally or analytically by applying seismic waves obtained from earthquakes such as El Centro, Ofunato, and Hachinohe to structures [24–27]. However, each real seismic wave has its own characteristics, which may cause different results depending on the natural frequency of the structure [28]. Therefore, in this study, artificial seismic loads were prepared using the seismic load generation method so as to be applicable to infrastructure proposed by the U.S.NRC, and the steps of the seismic load generation method suggested in the standard are as follows:

(1) The response spectra generated by the seismic load should cover the design response spectrum shown in Figure 3. However, for the frequency of up to five points, the response spectrum generated by the seismic load may have a smaller value than the design response spectrum;
(2) When the response spectrum of the seismic load is smaller than the design response spectrum, the value of the response spectrum of the seismic load shall not be less than 10% less than the value of the design response spectrum. In addition, even if the value is large, the value of the response spectrum of the seismic load should not be larger than 30% of the design response spectrum;
(3) The interval for generating the response spectrum is proposed in two cases, as follows:
    - When calculating spectrum values based on seismic loads, the frequency interval for calculating spectrum values must be sufficiently small. Table 1 shows the allowable frequency intervals for calculating the response spectrum using multiple damping ratios;
    - When calculating the spectral acceleration from the seismic load for a single damping ratio, the allowable frequency interval shall be calculated over 100 or more points of the frequency, with equal intervals on a log scale.

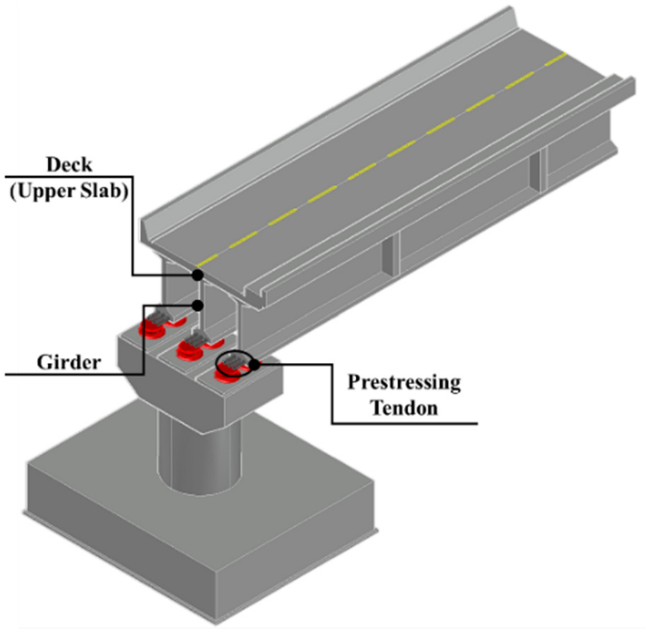

Figure 2. PSC girder bridge.

Table 1. Suggested frequency intervals for calculation of response spectra.

Frequency Range (Hz)	Increment (Hz)	Frequency Range (Hz)	Increment (Hz)
0.2~3.0	0.10	8.0~15.0	0.50
3.0~3.6	0.15	15.0~18.0	1.00
3.6~5.0	0.20	18.0~22.0	2.00
5.0~8.0	0.25	22.0~	3.00

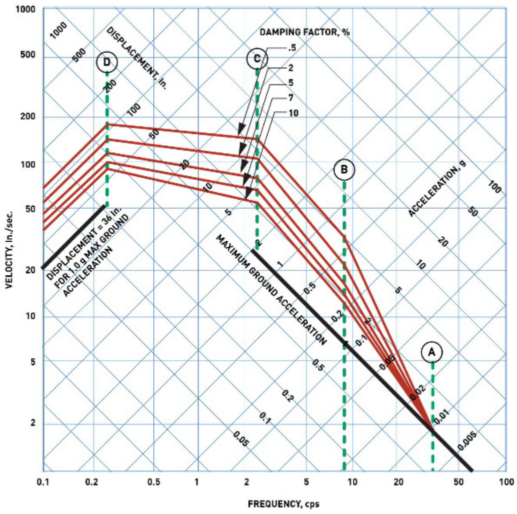

Figure 3. Horizontal design response spectra scaled to 1 g horizontal ground acceleration.

The artificial seismic load generated by SIMQKE—an artificial seismic load generation program—does not meet the criteria presented in the U.S. NRC standard. Lilhanand and Tseng [29] proposed a method of generating an artificial seismic load that is similar to the design response spectrum by applying a modification function, and verified that it affords sufficient reliability. Therefore, in this study, the seismic load generated in SIMQKE was modified using the modification function used in the prior study, and the modification function and modification time–history curve used in this study are as shown in Equations (1) and (2) and Figure 4.

$$f'(t) = \frac{-\omega_i}{\sqrt{1-\beta_i^2}} \exp(-\omega_i \beta_i (t_i - t)) \left(\left(2\beta_i^2 - 1 \right) \sin\left(\omega_i'(t_i - t)\right) - 2\beta_i^2 \sqrt{1-\beta_i^2} \cos\left(\omega_i'(t_i - t)\right) \right) \quad (1)$$

$$\omega_i' = \omega_i \sqrt{1-\beta_i^2} \quad (2)$$

where ω_i is the i-th natural frequency, β_i is the damping ratio, and t_i is the time at which the spectral response occurs.

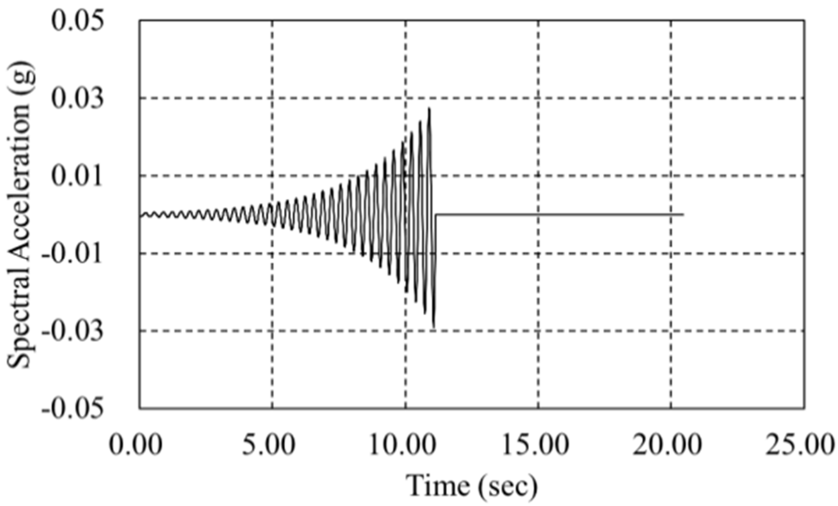

Figure 4. Time–history curve using modified function.

As shown in Figure 5, the seismic waves generated to meet the U.S.NRC standard are propagated to the ground surface throughout various soil layers. While the generated seismic wave is propagated to the ground surface, it can be amplified or diminished by reflecting the surrounding soil properties, and its characteristics can be changed [30–32]. To estimate the amplification of this seismic wave, the DEEPSOIL program [33] was employed in this study to perform a site response analysis. In the ground response analysis, the peak acceleration, shear deformation rate, shear wave velocity, and damping ratio of each soil layer were calculated, and the seismic load transferred to the free field was finally estimated.

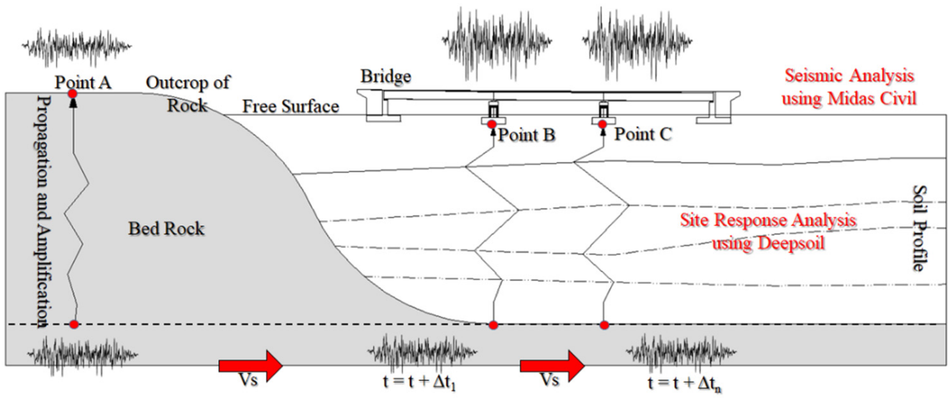

Figure 5. Propagation, amplification, and wave passage effect of seismic load.

The effect on the spatial variation of a seismic load is determined by wave passage and wave scattering, and the effect on the wave passage of the seismic load is determined by the shear wave velocity of the bedrock when the seismic load travels through the bedrock. Since the time difference occurs when the seismic load transmitted through the bedrock passes through the bedrock, the characteristics of the seismic load acting on the foundation of the structure change [34]. If the bedrock is very hard, the effect of the spatial variation of the seismic load can be negligible, because the seismic load travels very rapidly, but if it is located at considerable depth or it is not sufficiently hard, its effect should be considered. Therefore, in this study, seismic loads with a time difference of Δt were applied to the first pier (point B) and the second pier (Point C) of the PSC girder bridge, as shown in Figure 5. At this time, Δt was calculated based on the shear wave velocity of the bedrock.

3. Comparison of Seismic Load

In this study, the seismic response of PSC I-girder bridges under seismic load, considering the soil properties and wave passage effect, were investigated. To this end, the seismic loads acting on the bridges were first evaluated. The four seismic loads used in the evaluation are as below:

Seismic Load 1: El Centro record;
Seismic Load 2: Seismic load generated by SIMQKE;
Seismic Load 3: Seismic load generated by SIMQKE, modified to meet U.S. NRC standards;
Seismic Load 4: Seismic load considering the soil properties of the location where the bridge was installed using DEEPSOIL—a site response analysis program for seismic load modified to satisfy the USNRC.

3.1. Artificial Seismic Load

The artificial seismic load (called Seismic Load 1) and the response spectrum calculated from it are shown in Figure 6. Seismic Load 1 was generated with a total time of 20.48 s, a time interval of 0.005 s, and a peak acceleration of 0.30 g.

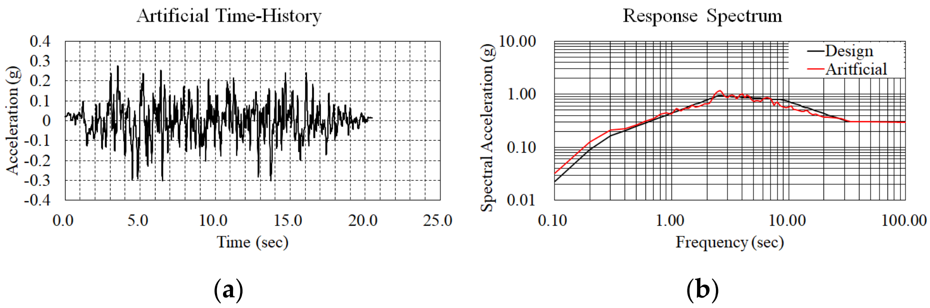

Figure 6. Initial time–history and response spectra: (**a**) initial time–history; (**b**) response spectrum using initial time–history.

When comparing the design response spectrum prepared by complying with the U.S. NRC standard and the response spectrum calculated by the Seismic Load 1, it was observed that the response spectrum was up to 45.0% larger than the design response spectrum in intervals below 1 Hz. Furthermore, the maximum value of the response spectrum of Seismic Load 1 was ~23.0% smaller than that of the design response spectrum between 10 Hz and 33 Hz. Therefore, in the case of a time–history analysis of bridges using Seismic Load 1, the possibility of over- or underevaluating the response depending on the natural frequency of the bridges should be taken into consideration.

3.2. Modified Artificial Seismic Load

The seismic load generated by SIMQKE was modified to meet the criteria presented in the U.S. NRC standard (Seismic Load 2), as shown in Figure 7a. A response spectrum was calculated using Seismic Load 2 and compared with the design response spectrum, as shown in Figure 7b. The modified seismic load using the modification function proposed by Lilhanand and Tseng [29] is the same as Seismic Load 1 in total time and time interval, and the peak acceleration is 0.301 g, confirming that it has approximately the same peak acceleration as Seismic Load 1. However, because the response spectrum produced from the modified seismic load is at least 0.08–26.0% larger than the design response spectrum at an interval of 0.01 Hz to 100 Hz, the response spectrum meets the design criteria. Therefore, when the time–history analysis of the bridge is performed using Seismic Load 2, the seismic load suggested in the design standard is considered to be acting on the bridge regardless of the natural frequency of the bridge.

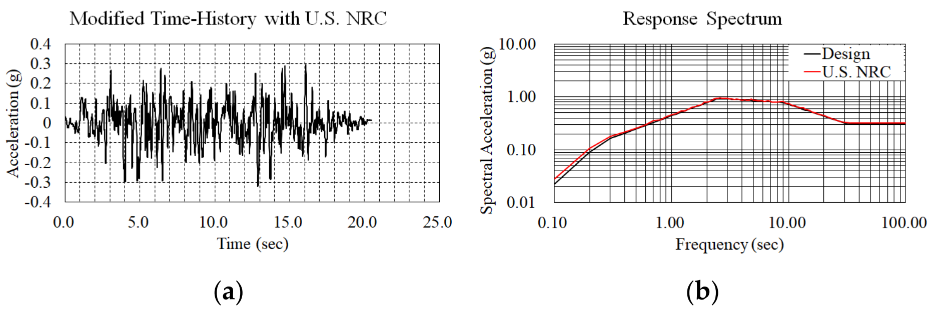

Figure 7. Modified time–history with U.S. NRC and response spectrum: (**a**) modified time–history; (**b**) response spectrum using time–history with U.S. NRC.

3.3. Modified Seismic Load Considering Soil Properties

The seismic loads from the bedrock to the ground surface can be amplified or diminished depending on the properties of the soil. Therefore, it is necessary to accurately estimate the seismic load transmitted to the ground surface by performing a ground response analysis that reflects the properties of the soil for the seismic load observed in the bedrock [35]. The location of the bridge considered in this study was randomly selected, and the soil properties at the bridge site referred to the study of Ahn et al. [35]. The ground consisted of granite weathered residual soil of ~5.0 m thickness, silt sand of ~7.0 m thickness, and a bedrock layer. The soil characteristics applied in the study are shown in Figure 8.

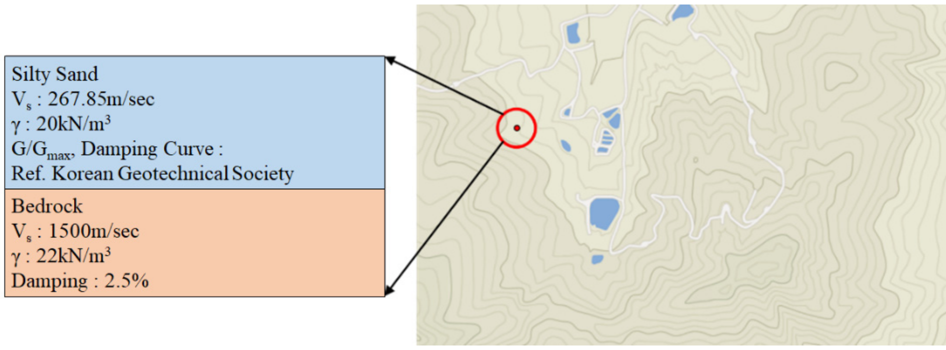

Figure 8. The soil type at the bridge's location.

In order to estimate the seismic load considering the soil properties of the bridge construction area, an equivalent linear seismic site response analysis was carried out. Equivalent linear ground response analysis is a linear analysis method that performs iterative calculations to consider the nonlinear dynamic properties of the soil, and was performed using the commercial program DEEPSOIL [35]. Considering the soil properties of the bridge's installation area, the seismic load with a peak acceleration of 0.301 g modified to meet the U.S. NRC (Seismic Load 2), as shown in Figure 9a, was amplified by ~35.0% and transformed into a seismic load with a peak acceleration of 0.406 g (Seismic Load 3). Furthermore, as shown in Figure 9b, the response spectrum between 0.4 Hz and 3.6 Hz increased by up to 170%, while the response spectrum between 3.6 Hz and 20 Hz decreased by up to 37%. These results indicate that even if the seismic load is prepared so as to meet the design criteria, the PSC girder bridge could be underestimated or overestimated because the properties of the seismic loads vary depending on the soil properties of the area where the bridge is constructed.

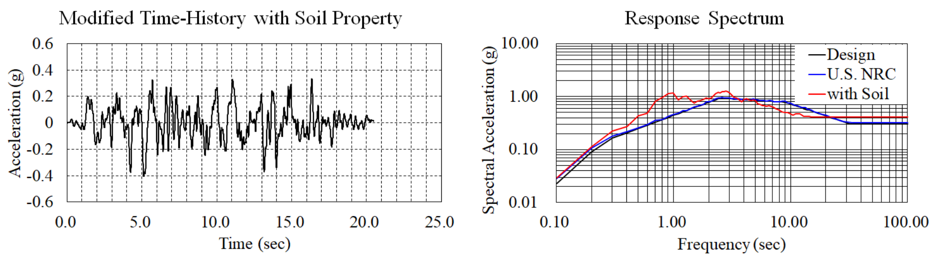

(**a**) (**b**)

Figure 9. Modified time–history with soil properties and response spectrum: (**a**) modified time–history with soil properties; (**b**) response spectrum using time–history with soil properties.

4. Discussion

This paper compared the seismic responses of the PSC girder bridge when subjected to the El Centro record (referred to as Seismic Load 1), the artificial seismic load generated by SIMQKE (Seismic Load 2), the artificial seismic load modified to meet the U.S. NRC design standard (Seismic Load 3), and the seismic load considering the soil properties (Seismic Load 4). In addition, the shear wave velocity of the bedrock, considering the soil properties and the wave passage effects, was used as a variable to estimate the seismic response of the bridge. The shear wave velocity of the bedrock was 500 m/s, 571 m/s, 667 m/s, 800 m/s, 1000 m/s, 1333 m/s, 2500 m/s, and 4000 m/s, and the wave passage effects were 0.08 s, 0.07 s, 0.04 s, 0.03 s, and 0.02 s.

4.1. FE Model for the PSC Girder Bridge

As shown in Figure 10a,c, the PSC I-girder bridge used in this study has three spans, where each span has a width of 12 m and a total length of 100 m, and the maximum inter-span distance is 40 m. The FE bridge model is detailed in Figure 10b,d,e. The FE model for I-girders, beams, and piers was built using beam elements, and the number of beam elements used was 331. Details of material constitutive models used for the I-girders, beams, and piers are shown in Table 2. The boundary conditions of the FE model are fixed at the abutment and the bottoms of the piers. Furthermore, in order to consider the bridge shoes installed at the connection of the bridge deck and the pier cap, the bridge deck and the pier cap were connected with a spring element.

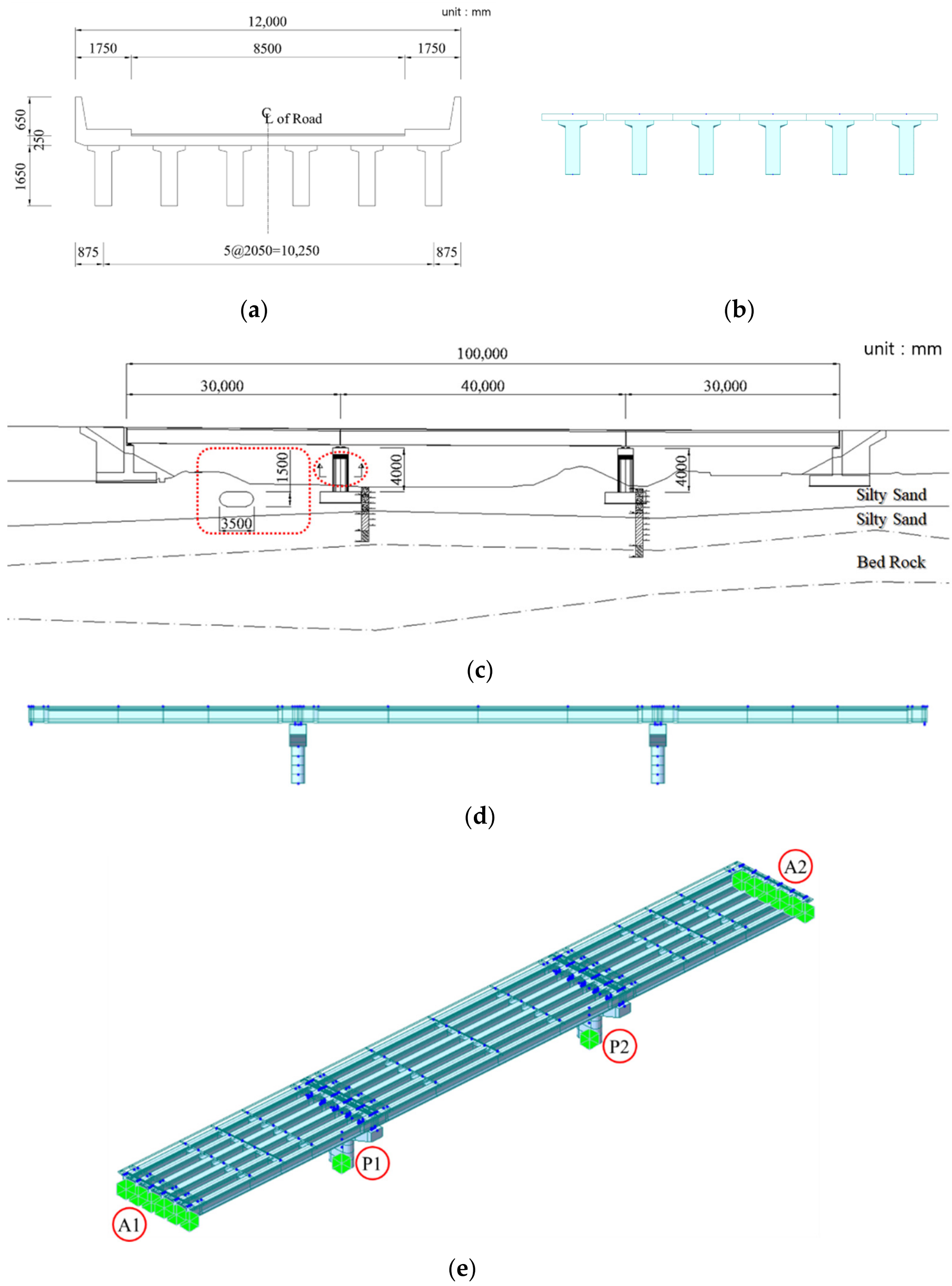

Figure 10. PSC girder bridge model for seismic analysis: (**a**) section properties; (**b**) section for the FE model; (**c**) side view of the PSC girder bridge; (**d**) side view of the PSC girder bridge for the FE model; (**e**) isometric view of the PSC girder bridge for the FE model.

Table 2. Material properties using the FE model.

	Compressive Strength (MPa)	Modulus of Elasticity (MPa)	Poisson's Ratio	Weight Density (kN/m^3)
Girder	35.0	29,755.0	0.18	24.5
Cross-Beam	24.0	26,964.0	0.18	24.5
Pier	21.0	26,094.0	0.18	24.5

4.2. Modal Analysis of the PSC Girder Bridge

The dynamic properties of the bridge were investigated by performing an eigenvalue analysis, and the results are shown in Figure 11 and Table 3. Figure 11c,e show the mode shapes of natural frequencies of 3.215 Hz and 5.428 Hz in the bridge's x-direction. Figure 11a,b show the mode shapes of natural frequencies of 1.784 Hz and 2.463 Hz in the bridge's y-direction. Figure 11d,f show the mode shapes of natural frequencies of 5.138 Hz and 20.389 Hz in the bridge's z-direction.

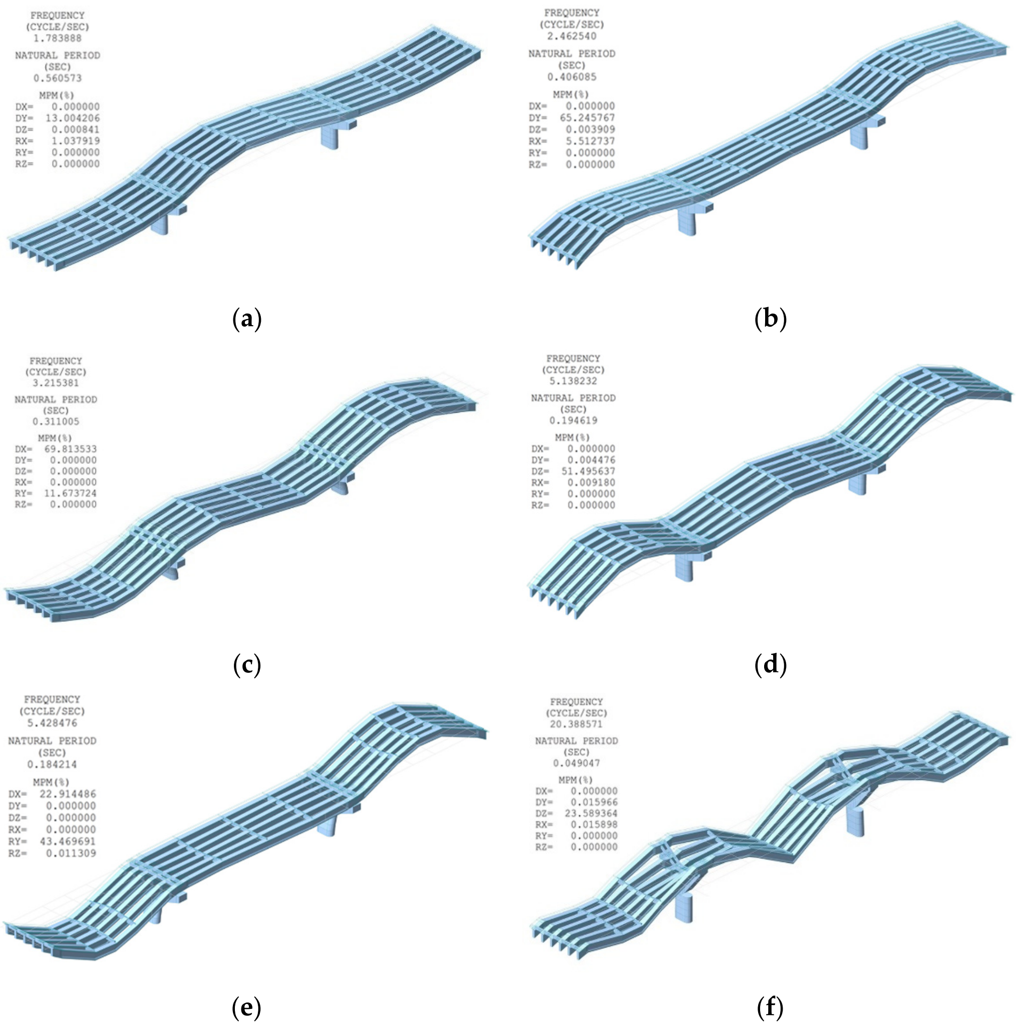

Figure 11. Mode shape, natural frequency, and mass participation at each translation: (**a**) Mode 1; (**b**) Mode 2; (**c**) Mode 4; (**d**) Mode 7; (**e**) Mode 8; (**f**) Mode 12.

Table 3. Natural frequency and mass participation.

Mode No.	Natural Frequency (Hz)	Mass Participation (%)		
		X-Translation	Y-Translation	Z-Translation
1	1.784	0.000	13.000	0.000
2	2.463	0.000	65.250	0.000
3	2.484	0.000	0.000	0.000
4	3.215	69.810	0.000	0.000
5	3.881	0.000	0.000	6.050
6	4.709	0.000	1.670	0.020
7	5.138	0.000	0.000	51.500
8	5.428	22.910	0.000	0.000
9	6.651	0.450	0.000	0.000
10	7.773	0.000	10.070	0.000
11	11.995	3.880	0.000	0.000
12	20.389	0.000	0.020	23.590

4.3. Seismic Response of the PSC Girder Bridge According to Seismic Properties

In the FE model of the bridge considered in this study, the seismic load in Figure 6a was acting on the x-translation of the bridge, and the acceleration response at the deck of the bridge was evaluated. In addition, the response spectrum was calculated using the seismic load acting on the bridge and the acceleration response on the deck of bridge generated by the corresponding seismic load. Figure 12 shows the response spectrum generated by the seismic load acting on the bottom of the foundation, as well as the acceleration response generated at the deck of the bridge. It can be seen that the response spectrum generated by the acceleration response of the deck of the bridge is amplified at 3.215 Hz, 5.428 Hz, and 11.995 Hz, which are the natural frequencies of the 1st, 2nd, and 3rd modes in the x-direction of the bridge, respectively. This is because the response acceleration of the bridge is amplified by resonance in the natural frequency in the x-direction of the structure.

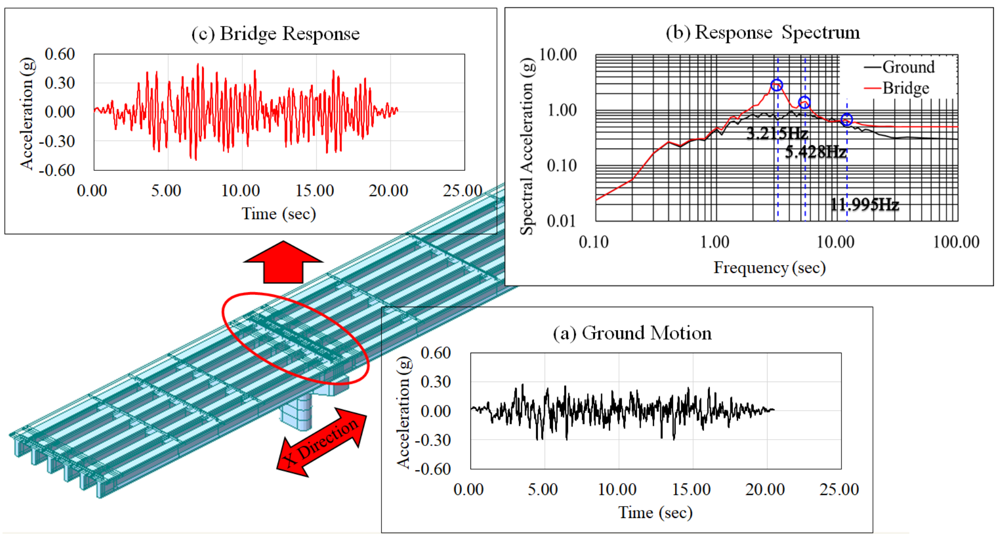

Figure 12. Time–history and response spectrum: (**a**) modified time–history with soil properties; (**b**) response spectrum using time–history with soil properties; (**c**) response time-history at the deck of the bridge.

The response of acceleration and the maximum bending moment at the ground and deck of the bridge are shown in Figure 13 and Tables 4 and 5 for when Seismic Load 1, Seismic Load 2, Seismic Load 3, and Seismic Load 4 are acting on the PSC I-girder bridge. The peak acceleration of each seismic load was 0.357 g for Seismic Load 1, 0.300 g for Seismic Loads 2 and 3, and 0.406 g for Seismic Load 4. The maximum bending moments of the bridge under Seismic Loads 2 and 3, with the same peak acceleration of 0.300 g, were 2308.36 kN·m and 3223.90 kN·m, respectively, showing a difference of ~139%. It was confirmed that different member forces can be calculated according to the response spectrum acceleration of the natural frequency of the bridge under the seismic load of the same peak acceleration. Therefore, it was observed that even with identical acceleration for the seismic load, member forces depend on the seismic load and the natural frequency of the bridge. The response acceleration of the bridge was compared when Seismic Loads 1 and 3 were applied. From the results, Seismic Load 1 had a ~119% higher maximum response acceleration than Seismic Load 3, but the latter had a ~120% higher maximum bending moment than Seismic Load 1. This phenomenon might take place because, as mentioned above, the seismic load and natural frequency of the bridge affect the results.

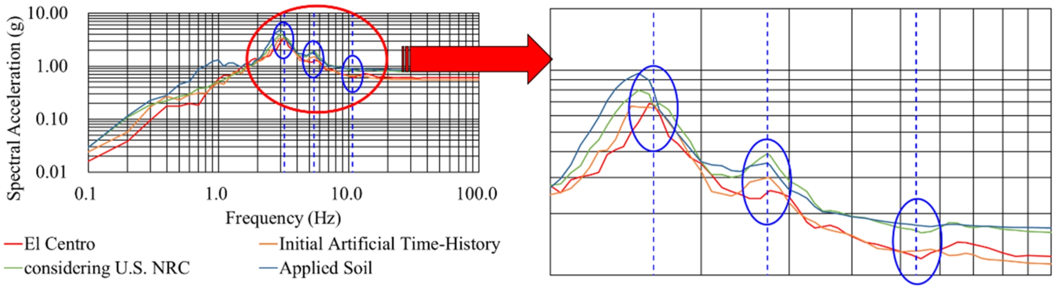

(**a**)

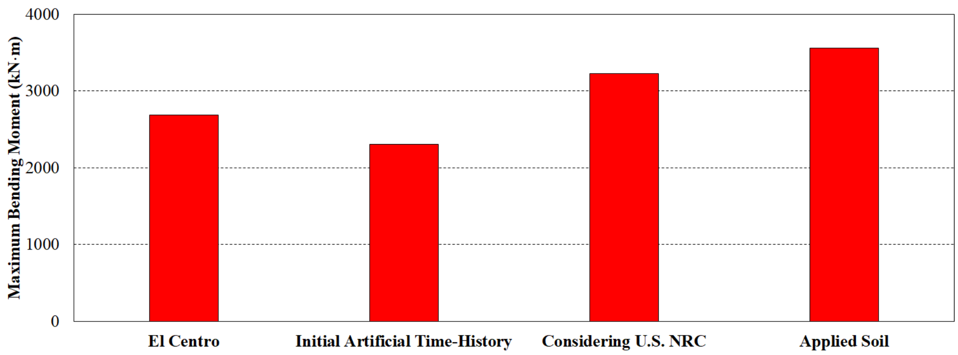

(**b**)

Figure 13. Comparison of response spectrum and maximum bending moment at each seismic load: (**a**) response spectrum of the PSC girder bridge; (**b**) maximum bending moment.

Table 4. Comparison of peaked acceleration and spectral acceleration at ground.

Seismic Load	Peaked Acceleration	Spectral Acceleration		
		1st Mode	2nd Mode	3rd Mode
El Centro	0.357	0.732	0.739	0.561
Initial Artificial Time–History	0.300	0.670	0.823	0.581
Considering U.S. NRC	0.300	0.867	0.868	0.655
Applied Soil	0.406	1.009	0.728	0.464

Table 5. Comparison of peaked acceleration, spectral acceleration, and maximum bending moment of the PSC girder bridge.

Seismic Load	Peaked Acceleration	Ratio (%)	Spectral Acceleration						Maximum Bending Moment (kN·m)
			1st Mode	Ratio (%)	2nd Mode	Ratio (%)	3rd Mode	Ratio (%)	
El Centro	0.609	170.588	3.387	462.705	1.268	171.583	0.615	109.626	2683.60
Initial Artificial Time–History	0.549	183.000	3.275	488.806	1.499	182.139	0.658	113.253	2308.36
Considering U.S. NRC	0.782	260.667	3.302	380.854	1.955	225.230	0.826	126.107	3223.90
Applied Soil	0.836	205.911	3.954	391.873	1.762	242.033	0.880	189.655	3561.83

Comparing the member forces under the four seismic loads applied to the bridge, the seismic load considering the soil properties had the greatest maximum bending moment among the seismic loads, at 3561.83 kN·m. This is because the peak acceleration acting on the ground, the response spectrum acceleration calculated from the natural frequency of the bridge, and the response acceleration generated from the bridge all have large values compared to other seismic loads. Therefore, in order to ensure the safety of the bridge considering the uncertainty of the seismic load, it is necessary to take into account the soil properties of the area in which the bridge is constructed, while complying with the seismic design code.

4.4. Seismic Response of the PSC Girder Bridge According to the Wave Passage Effect

Assuming the bedrock shear wave velocity of Seismic Load 4 as 500 m/s, 571 m/s, 667 m/s, 800 m/s, 1000 m/s, 1333 m/s, 2500 m/s, and 4000 m/s, and applying wave passage effect as 0.08 s, 0.07 s, 0.06 s, 0.05 s, 0.04 s, 0.03 s, 0.02 s, and 0.01 s, respectively, the seismic response of the bridge was compared, as shown in Figure 14 and Table 6. We observed that insignificant differences appeared in the maximum bending moment during the increase in the wave passage effect from 0.00 s to 0.05 s. However, after 0.06 s, the maximum bending moment dramatically increased, and it was confirmed that the maximum bending moment increased by ~150% at 0.08 s compared to 0.06 s.

Table 6. Comparison of peaked acceleration, spectral acceleration, and maximum bending moment of the PSC girder bridge.

Wave Passage Effect	Peaked Acceleration	Spectral Acceleration			Max. Bending Moment (kN·m)
		1st Mode	2nd Mode	3rd Mode	
ΔT: 0.00 s	0.836	3.954	1.762	0.880	3561.83
ΔT: 0.01 s	0.835	3.950	1.757	0.879	3605.90
ΔT: 0.02 s	0.830	3.917	1.729	0.873	3638.98
ΔT: 0.03 s	0.833	3.936	1.746	0.877	3626.76
ΔT: 0.04 s	0.803	3.748	1.588	0.848	3635.79
ΔT: 0.05 s	0.782	3.614	1.479	0.828	3637.15
ΔT: 0.06 s	0.758	3.448	1.347	0.803	4009.57
ΔT: 0.07 s	0.730	3.253	1.196	0.773	4675.18
ΔT: 0.08 s	0.698	3.029	1.028	0.739	5344.66

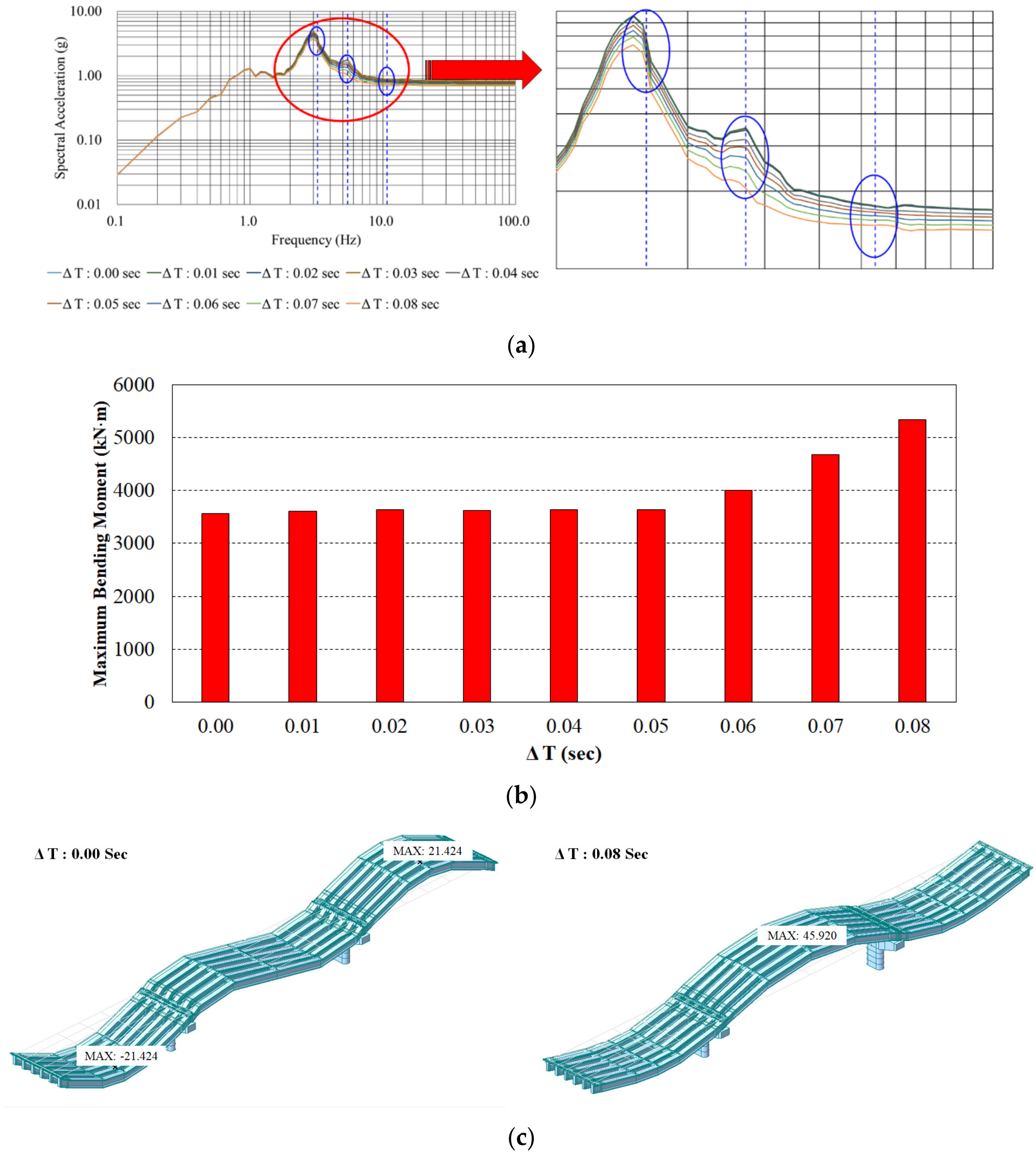

Figure 14. Comparison of response spectrum and maximum bending moment considering the wave passage effect: (**a**) response spectrum of the PSC girder bridge; (**b**) maximum bending moment; (**c**) deformation shape.

The response spectrum calculated from the response acceleration of the bridge shows small differences in the 1st, 2nd, and 3rd modes of the bridge, until 0.04 s of the wave passage effect. However, from 0.05 s, the response spectrum began to decrease in the major mode of the bridge, and in the 2nd mode of 0.08 s of the wave passage effect it reduced by ~58% compared to the 2nd mode of 0.00 s. This is because even if identical seismic loads act on the bridge, the acceleration in the opposite direction acts on the two piers due to the wave passage effect, as can be confirmed by the displacement shape of the deck of the bridge shown in Figure 14c. Based on the above results, to ensure the stability of the bridge under seismic loads, the wave passage effect should be considered under a shear wave velocity of bedrock of 1000 m/s (Δt: 0.05 s) in the area where the bridge is constructed.

5. Conclusions

In this study, the seismic response of a PSC I-girder bridge under seismic loads, considering the soil properties and the wave passage effect, was investigated. The seismic response of a PSC I-girder bridge was analyzed using the El Centro record, an artificial seismic load generated by SIMQKE, a seismic load modified to meet the U.S. NRC standard, and a seismic load considering the soil properties of the area where the bridge was constructed using the DEEPSOIL program.

The peak acceleration of the four seismic loads was 0.357 g, 0.300 g, 0.300 g, and 0.406 g, respectively, while the maximum response acceleration of the bridge was 0.609 g, 0.549 g, 0.782 g, and 0.836 g, respectively. In addition, the maximum bending moment in the bridge was calculated to be 2308.36 kN·m and 3223.90 kN·m, respectively, under two seismic loads with the same peak acceleration of 0.300 g, which was confirmed to have a difference of ~139%. The response acceleration calculated for the bridge when the real seismic load (El Centro) and the seismic load modified to meet the U.S. NRC standard were applied was compared. The real seismic load (El centro) had a ~119% larger maximum response acceleration than the seismic load modified to meet the U.S NRC standard, but the maximum bending moment of the real seismic load (El Centro) was ~120% greater than that of the seismic load modified to meet the U.S NRC.

The behavior of the PSC girder bridge was analyzed by considering the shear wave velocity for seismic loads and considering the soil properties. After the wave passage effect of 0.06 s, the maximum bending moment dramatically increased, and at the wave passage effect of 0.08 s, a roughly 150% maximum bending moment appeared. When the wave passage effect was 0.05 s, the response spectrum calculated from the response acceleration from the bridge decreased in the 1st, 2nd, and 3rd modes of the bridge, and the response spectrum at the 2nd mode of the wave passage effect at 0.08 s had ~58% of the response spectrum compared to the 2nd mode of 0.00 s.

Therefore, in order to ensure the safety of the bridge, considering the uncertainty of the seismic load, it is necessary to take into account the soil properties of the area in which the bridge is constructed, while complying with the seismic load design code. In addition, the wave passage effect calculated using the shear wave velocity of the bedrock in the area where the bridge is constructed should be considered in order to ensure the earthquake resistance of the bridge.

However, for the seismic loads applied in this study, it was assumed that the soil properties of the area where the bridge is installed were the same at all points, because the DEEPSOIL and ProShake programs, which are currently in use, apply a one-dimensional equivalent linear seismic site response analysis. The site response analysis program can consider the soil properties in the area where the bridge is constructed according to depth, but it cannot consider the soil properties converted to the horizontal direction. Therefore, in order to confirm the dynamic behavior of the bridge as being similar to that of the real one, it is considered that additional research on the response analysis of the two-dimensional equivalent linear site should be conducted.

In addition, the transmission speed of seismic load transmitted to the bridge varies depending on the wave passage effect transmitted from bedrock, the depth of ground, and the characteristics of each stratum. It is therefore necessary to further study the transmission speed of seismic load, depending on the depth of the ground and the characteristics of the stratum.

Author Contributions: Conceptualization, Y.-M.Y. and G.P.; data curation, Y.-M.Y. and K.-N.H.; investigation, Y.-M.Y. and S.L.; supervision, G.P.; writing—original draft preparation, Y.-M.Y. and G.P.; writing—review and editing, S.L. and K.-N.H. All authors have read and agreed to the published version of the manuscript.

Funding: This research received no external funding.

Institutional Review Board Statement: Not applicable.

Data Availability Statement: Not applicable.

Conflicts of Interest: The authors declare no conflict of interest.

References

1. Kwon, H.-J.; Yang, K.-H.; Sim, J.-I. Proposals of Reliable Shapes of Supplementary V-Ties for Section Jacketing Method of Columns. *J. Korea Inst. Build. Constr.* **2018**, *18*, 99–107.
2. Dong, J.-F.; Wang, Q.-Y.; Guan, Z.-W. Material properties of basalt fiber reinforced concrete made with recycled earthquake waste. *J. Constr. Build. Mater.* **2017**, *130*, 241–251. [CrossRef]
3. Testuya, S.; Masayasu, O. Damage estimation of concrete canal due to earthquake effects by acoustic emission method. *J. Constr. Build. Mater.* **2014**, *67*, 186–191.
4. Lee, K.-S.; Yi, W.-H.; Lew, H.-S. Nonlinear Seismic Analysis Method of Reinforced Concrete Buildings Including Their Pile Foundations. *J. Earthq. Eng. Soc. Korea* **2003**, *7*, 9–20.
5. Abdel Raheem, S.E.; Ahmed, M.M.; Alazrak, T.M.A. Evaluation of soil–foundation–structure interaction effects on seismic response demands of multi-story MRF buildings on raft foundations. *Int. J. Adv. Struct. Eng.* **2014**, *7*, 11–30. [CrossRef]
6. Wang, H.; Lou, M.; Chen, X.; Zhai, Y. Structure–soil–structure interaction between underground structure and ground structure. *Soil Dyn. Earthq. Eng.* **2013**, *54*, 31–38. [CrossRef]
7. Lysmer, J.; Udaka, T.; Tsai, C.; Seed, H.B. *FLUSH-A Computer Program for Approximate 3-D Analysis of Soil-Structure Interaction Problems*; California University: Los Angeles, CA, USA, 1975.
8. Wolf, J.P. Soil-structure-interaction analysis in time domain. In *Structural Mechanics in Reactor Technology*; IAEA: Vienna, Austria, 1987.
9. Avilés, J.; Pérez-Rocha, L.E. Soil–Structure Interaction in Yielding Systems. *Earthq. Eng. Struct. Dyn.* **2003**, *32*, 1749–1771. [CrossRef]
10. Wolf, J.P.; Song, C. Some Cornerstones of Dynamic Soil–Structure Interaction. *Eng. Struct.* **2002**, *24*, 13–28. [CrossRef]
11. Jardine, R.J.; Potts, D.M.; Fourie, A.B.; Burland, J.B. Studies of the Influence of Non-Linear Stress–Strain Characteristics in Soil–Structure Interaction. *Geotechnique* **1986**, *36*, 377–396. [CrossRef]
12. Mohanty, P.; Dan, X.; Biswal, S.; Bhattacharya, S. A shake table investigation of dynamic behavior of pile supported bridges in liquefiable soil deposits. *Earthq. Eng. Eng. Vib.* **2021**, *20*, 1–24. [CrossRef]
13. Kwon, J.-S.; Paik, I.-Y.; Chang, S.-P. Dynamic Analysis of Floating Bridge subject to Earthquake Load Considering Multi-Support Excitation. *J. Earthq. Eng. Soc. Korea* **2004**, *8*, 27–33.
14. Ohsaki, M. Sensitivity of Optimum Designs for Spatially Varying Ground Motions. *J. Struct. Eng.* **2001**, *127*, 1324–1329. [CrossRef]
15. Ancheta, T.D.; Stewart, J.P.; Abramhamson, N.A. Engineering characterization of earthquake ground motion coherency and amplitude variability. In Proceedings of the 4th International Symposium on Effects of Surface Geology on Seismic Motion, University of California, Santa Barbara, CA, USA, 23–26 August 2011; IASPEI/IAEE: Santa Barbara, CA, USA, 2011.
16. Kim, I.-T.; Han, J.-W.; Yun, S.; Park, D.-H. Prediction of Tunnel Response by Spatially Variable Ground Motion. *J. Korean Geo-Environ. Soc.* **2008**, *9*, 53–61.
17. Kim, Y.-S.; Roesset, J.M. Effect of Nonlinear Soil Behavior on the Inelastic Seismic Response of a Structure. *Int. J. Geomech. ASCE* **2004**, *4*, 104–114. [CrossRef]
18. Kim, Y.-S. Wave Passage Effect on the Seismic Response of a Building Considering Bedrock Shear Wave Velocity. *J. Earthq. Eng. Soc. Korea* **2014**, *18*, 89–94. [CrossRef]
19. Shamsabadi, A.; Rollins, K.M.; Kapuskar, M. Nonlinear Soil–Abutment–Bridge Structure Interaction for Seismic Performance-Based Design. *J. Geotech. Geoenviron. Eng.* **2007**, *133*, 707–720. [CrossRef]
20. Wang, Z.; Dueñas-Osorio, L.; Padgett, J.E. Seismic Response of a Bridge–Soil–Foundation System under the Combined Effect of Vertical and Horizontal Ground Motions. *Earthq. Eng. Struct. Dyn.* **2013**, *42*, 545–564. [CrossRef]
21. Chen, W.; Huang, G. Seismic Wave Passage Effect on Dynamic Response of Submerged Floating Tunnels. *Procedia Eng.* **2010**, *4*, 217–224. [CrossRef]
22. Adanur, S.; Altunışık, A.C.; Başağa, H.B.; Soyluk, K.; Dumanoğlu, A.A. Wave-Passage Effect on the Seismic Response of Suspension Bridges Considering Local Soil Conditions. *Int. J. Steel Struct.* **2017**, *17*, 501–513. [CrossRef]
23. Bayraktar, A.; Hokelekli, E. Nonlinear soil deformability effects on the seismic damage mechanisms of brick and stone masonry arch bridge. *Int. J. Damage Mech.* **2021**, *30*, 431–452. [CrossRef]
24. Ling, S.; Chigira, M. Characteristics and Triggers of Earthquake-Induced Landslides of Pyroclastic Fall Deposits: An Example from Hachinohe during the 1968 M7. 9 Tokachi-Oki Earthquake, Japan. *Eng. Geol.* **2020**, *264*, 105301. [CrossRef]
25. Takao, T.; Kozawa, K.; Murakami, K.; Abe, I.; Ogasawara, T.; Shibaki, H.; Nakamura, Y. Impact on Dissolved Oxygen of Intermittent Deep Water Intrusion from the Outer Bay after the 2011 Tohoku Earthquake Tsunami in Ofunato Bay, Japan. In *Proceedings of the ASIAN AND PACIFIC COASTS 2017: Proceedings of the 9th International Conference on APAC 2017*; World Scientific: Pasay City, Philippines, 2018; pp. 882–893.
26. Matsuoka, K.; Ikeda, Y.; Kaga, S.; Kaga, Y.; Ogata, T. Repercussions of the Great East Japan Earthquake Tsunami on Ellipsoidal Alexandrium Cysts (Dinophyceae) in Ofunato Bay, Japan. *Mar. Environ. Res.* **2018**, *135*, 123–135. [CrossRef] [PubMed]
27. Amirchoupani, P.; Abdollahzadeh, G.; Hamidi, A. Improvement of energy damage index bounds for circular reinforced concrete bridge piers under dynamic analysis. *Struct. Concr.* **2021**, *22*, 3315–3335. [CrossRef]
28. Park, G.; Hong, K.N.; Han, S.H.; Kim, J.S. Generation of Artificial Time History Covering Design Response Spectrum by Two Modification Functions. *J. Korean Soc. Civ. Eng.* **2016**, *36*, 1–11. [CrossRef]

29. Lilhanand, K.; Tseng, W.S. Development and Application of Realistic Earthquake Time Histories Compatible with Multiple-Damping Design Spectra. In Proceedings of the 9th World Conference on Earthquake Engineering, Tokyo, Japan, 2–9 August 1988; Volume 2, pp. 819–824.
30. Newmark, N.M.; Hall, W.J. Earthquake Spectra and Design. In *Engineering Monographs on Earthquake Criteria*; Earthquake Engineering Research Institute: Berkeley, CA, USA, 1982.
31. Hudson, D.E. *Reading and Interpreting Strong Motion Accelerograms*; Earthquake Engineering Research Institute: Berkeley, CA, USA, 1979; Volume 1.
32. Seed, H.B.; Ugas, C.; Lysmer, J. Site-Dependent Spectra for Earthquake-Resistant Design. *Bull. Seismol. Soc. Am.* **1976**, *66*, 221–243. [CrossRef]
33. Hashash, Y.M.A.; Musgrove, M.I.; Harmon, J.A.; Okan, I.; Xing, G.; Numanoglu, O.; Groholski, D.R.; Phillips, C.A.; Park, D. DEEPSOIL 7.0, User Manual. Board of Trustees of University of Illinois at Urbana-Champaign: Urbana, IL, USA, 2020. Available online: http://deepsoil.cee.illinois.edu (accessed on 25 December 2021).
34. Ancheta, D.T. Engineering Characterization of Spatially Variable Earthquake Ground Motions. Ph.D. Thesis, University of California, Los Angeles, CA, USA, 2010; 220p.
35. Ahn, S.; Ahn, K.; Lee, C.; Lee, J.-D.; Jung, J. Evaluation of Dynamic Properties and Ground-Response Analysis of Soil Reinforced with Cement and Biopolymer. *J. Korean Soc. Hazard Mitig.* **2020**, *20*, 291–296. [CrossRef]